



On the combined effect of topographic irregularities and wave passage on the spatial variation of seismic ground motion

M. G. Durante¹ · S. J. Brandenburg² · E. Ausilio¹ · P. Zimmaro^{3,2}

Received: 31 July 2021 / Accepted: 29 November 2021 / Published online: 5 January 2022
© The Author(s), under exclusive licence to Springer Nature B.V. 2021

Abstract

The spatial variation of ground motion (SVGGM) can significantly affect the response of distributed infrastructure systems including bridges, dams, and pipelines. SVGGM-related phenomena are the result of the combination of three effects: (1) wave passage, (2) geometric incoherence of the input, and (3) ground- and site-effects due to soil layering, the presence of topographic irregularities, and/or alluvial basins. Existing models are able to capture wave passage and geometric incoherence effects, while ground- or site-effects are either not modeled, or treated in a simplified manner. We perform a numerical experiment by means of the finite element method, exploring the combined effect of wave passage and the presence of 2D topographic features. Such combined effects were observed following recent earthquakes, but were never analyzed using a comprehensive set of numerical analyses. We explore two regularly shaped canyons (semi-circular and V-shaped) and a real case study for a canyon crossed by a multi-span bridge in Italy: the Viadotto Italia. We show that the combined effect of wave passage and topographic features can modify the amplitude and shape of the input motion, altering soil-structure interaction processes involving bridge piers. We also show that path effects, related to the direction of the input motion, have an influence on how input ground motions are modified. For all canyon shapes explored, there is a significant amplification of the vertical component of the motion that sometimes becomes comparable to the horizontal components. We anticipate that outcomes from this research would improve future engineering models and/or site-specific studies.

Keywords Wave passage effect · Topographic effects · Topographic irregularities · Spatial variation of ground motion · Multi-span bridges

✉ M. G. Durante
mgdurante@unical.it

¹ Department of Civil Engineering, University of Calabria, Via P. Bucci,
87036 Arcavacata di Rende, Italy

² Department of Civil and Environmental Engineering, University of California, Los Angeles, 5731
Boelter Hall, Los Angeles, CA 90095-1593, USA

³ Department of Environmental Engineering, University of Calabria, Via P. Bucci,
87036 Arcavacata di Rende, Italy

1 Introduction

Routine numerical one-dimensional (1D; ground response) and two- or three-dimensional (2D or 3D) seismic site response applications typically neglect the effects of the spatial variation of ground motion (SVGGM). As a result, such numerical models assume a synchronous motion at the base of the model. This assumption may be acceptable in the case of structures of limited spatial extent, where site conditions can be treated as 1D wave propagation problems. In case of long structures and distributed infrastructure systems, such as bridges, dams, tunnels, and pipelines, the actual ground motion varies significantly along the base of the system, generating non-negligible variations in terms of amplitude and phase of the motion. This phenomenon is currently well recognized in the literature, but its quantitative analysis is not trivial and its effects still not well-characterized. This problem can be simplified by breaking down the problem into separate components, where different modifiers (one for each component of the phenomenon) are applied to the input motion. This can be done by assuming that the asynchronous motion can be considered as the combination of three effects: (i) wave passage (due to the finite propagation velocity of seismic waves, resulting in progressive excitation as a wave front passes); (ii) geometric incoherence of the input (it accounts for wave scattering effects due to inhomogeneity of soil, that change the signal contents); (iii) local ground- and site- response effects (it includes 1D, 2D, and 3D effects). Topographic effects can be treated as either 2D or 3D effects (depending on the shape of the topographic feature being analyzed) and included in the latter term. Several studies, using data from recent earthquakes, observed significant variations of amplitude and phase of a motion due to the combination of wave passage, geometric incoherence and ground- and site-response effects (e.g., Davis and West 1973; Siro 1982; Celebi and Hanks 1986; Assimaki and Gazetas 2004; Assimaki and Jeong 2013; Capatti et al. 2016).

Over the last decades, several studies showed how earthquake-induced damage to long infrastructure systems, such as bridges and tunnels, can seriously compromise their use and functionality, even when designed according to relatively modern seismic codes (Elanashai et al. 1999). Most of the time, the poor performance of these structures was associated with the detrimental effects of the SVGGM (Sextos et al. 2003; Lupoi et al. 2005; Park et al. 2009). One of the first models proposed to quantify the SVGGM was developed by Vanmarcke (1983) who used for the first time a probabilistic approach based on the random field theory, while Zerva (1990) introduced the idea of using random signals as input. Another well-known method was developed by Luco and Wong (1986), who proposed a simplified approach to generate seismic inputs based on the motion selected at the first point of the model. Recently, more complex methodologies were developed (Sextos et al. 2003, 2005; Nuti and Vanzi 2005). Interestingly, Sextos et al. (2003) proposed a methodology to evaluate the seismic response of bridges including soil-structure interaction and site effects in a simplified manner. The limitation of this method is that site effects are computed using 1D simulation, neglecting 2D and 3D topographic effects. As a result, none of the currently available methods explicitly model all components of the problem. Typically, wave passage and geometric incoherence effects are modeled, leaving out, or using simplified 1D models to account for site effects. The complexities associated with the development of an accurate model that includes site effects due to topographic irregularities certainly represent a significant obstacle to their inclusion in simplified/pragmatic engineering models.

Site response due to topographic irregularities is strictly related to the geometric characteristics of the topographic feature (e.g., ridges, slopes, and canyons). The response of a half-space semi-circular canyon formed by an elastic, homogeneous, and isotropic material was studied by Trifunac (1973) and Wong (1982). For the first time, they analyzed wave propagation effects due to topographic irregularities for SH, P, and SV incident waves. Subsequently, under the same hypotheses, Godinho et al. (2009) computed the surface displacement along regularly-shaped canyons using the method of fundamental solutions (MFS). More recently, Wu et al. (2016) presented an improved methodology to include topographic effects in the definition of asynchronous motions for sites located in V-shaped canyons.

In this paper, we present the effects of the SVGM on two regular topographic features: semi-circular and V-shaped canyons and for a real canyon overcrossed by a long multi-span bridge in Southern Italy (the Viadotto Italia crossing the Lao River in the Calabria region). We perform a large number of numerical simulations including wave passage and site effects due to topographic irregularities. The goal of this study is to explore the extent to which the combination of these effects (often neglected in practice) modifies the ground surface motion and how such effects are influenced by the shape of the topographic feature and various characteristics of the input motion. A preliminary analysis of the case study that did not include wave passage effects, was presented by Durante et al. (2018). In this study, wave passage effects are modelled adding a delay to the arrival times of seismic waves at different locations, while local site effects (i.e., topographic features) are included in an ad-hoc geotechnical model using a two-dimensional finite element method (FEM) model, developed using the software framework OpenSees (McKenna and Fenves 2005). Our numerical model was first verified against known analytical solutions available from literature for regularly-shaped canyons. A second verification study was conducted for the Lao River canyon comparing our FEM implementation against a previously verified numerical model based on the boundary element method (BEM) (Ausilio et al. 2008; Ausilio and Zimmaro 2012). After the verification study, a parametric analysis was performed for each of three canyon shapes (i.e., semi-circular, V-shaped, and the Lao River canyon), using sinusoidal SV waves with three different values of dimensionless frequencies (i.e., a representative quantity accounting for the shape and stiffness of the canyon), each of which with increasing severity of wave passage effects. The effect of the direction of the input was explored, considering seismic waves coming from left to right, and from right to left. Wave directions can be used as a proxy for the direction of the causative fault of an earthquake with respect to the site being analyzed.

To the best of our knowledge, this is the first time that wave passage effects and topographic irregularities are analyzed in tandem in a comprehensive numerical program. Results from this study are reported in terms of horizontal and vertical aggravation factors along the canyon surfaces. We anticipate that results from this study would inform both: (1) simplified/pragmatic engineering frameworks, and (2) future site-specific studies involving the analysis of complex multi-span bridges crossing topographic features. Such insights would also be informative for advanced fully-coupled soil-structure interaction studies.



Fig. 1 Overview of the Viadotto Italia (Durante et al. 2018)

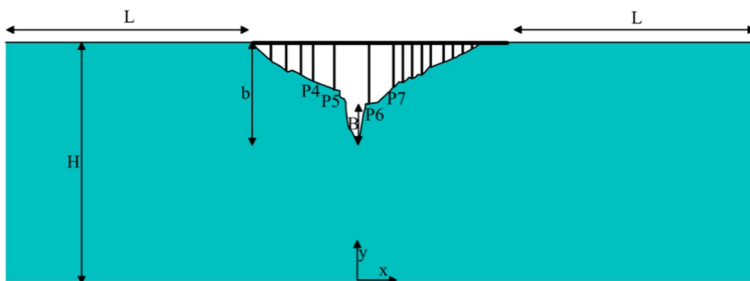


Fig. 2 Schematic view of the analyzed cross-section [adapted from Durante et al. (2018)]

2 The Viadotto Italia case study

In addition to two regularly-shaped canyons (presented in a subsequent section), the case study considered in this paper is a 260 m-deep canyon on the Lao River overcrossed by a 1160 m-long multi-span-bridge: the Viadotto Italia in the Calabria region (Southern Italy) along the A2 Mediterranean highway (Fig. 1). The Viadotto Italia is located between the towns of Laino Castello and Laino Borgo in the Cosenza province, a highly seismic area. The bridge was built in the 1960s and it is currently the second highest bridge in Europe, after being the highest in Europe in the period 1974–2004. The bridge was the object of several studies because of its importance and complexity. Its design and construction represented an engineering challenge for the time (Cestelli Guidi et al. 1965) and it still represents an important landmark for the whole area. The original bridge was formed by 19 spans, 17 piers, and 2 abutments. Its peculiarity was the central part, formed by three long steel spans (125, 175, and 125 m), connected to the other parts by means of curved prestressed concrete spans. The piers are formed by hollow sections tapered along the height. In recent years, the bridge was renovated to align it with more recent safety standards. During this renovation process the original bridge was kept in the central part, while the curved parts were substituted by straight spans. As a result of this modifications, the number and the position of some piers changed over the years.

In this study, we modeled the 2D cross-section crossed by the new configuration of the viaduct (Fig. 2), for which detailed information on the stratigraphy of the soil deposit are available from in situ tests including boring logs and geophysical tests. In the present study,

the complex stratigraphy of the area is not included, and the deposit is modeled using an elastic and homogeneous soil deposit, assuming a shear wave velocity, $V_s = 500$ m/s and a Poisson ratio, $\nu = 0.33$. The bridge is not modeled in the analyses, but the locations of the piers are used as reference points in the discussion of the results. We decided to remove any stratigraphic complexities to explore the coupled effect of wave passage and topographic irregularities. The inclusion of additional variables (i.e., the stratigraphy) would have impaired our ability to decouple each effect and identify which effect causes what consequences.

3 Numerical model

The open-source software OpenSees (McKenna and Fenves 2005) is used to perform 2D FEM analysis of two regularly-shaped canyons (semi-circular and V-shaped) and the Lao river canyon case study schematically represented in Fig. 2. The soil domain is modelled considering plain strain conditions. The domain was discretized using four-node, bilinear, isoparametric finite elements with four point of integration for each of them. Absorbing Lysmer type boundaries are implemented by means of a set of viscous dampers normal and tangential to the soil boundaries (Lysmer and Kuhlemeyer 1969). Detailed information about the implementation of this approach are available in Zhang et al. (2003).

The dynamic input is defined at each node of the base of the domain in terms of equivalent nodal forces proportional to the velocity of the seismic wave and the tributary surface area of each element. The input is applied in the horizontal direction to simulate vertically incident SV-waves, and a delay is added to the arrival time of the input motion to include the wave passage effect. The delay is computed using the following relationship:

$$\Delta t = \frac{\Delta h}{V_s \lambda_{app} / \lambda_{soil}} \quad (1)$$

where Δh is the distance between nodes, $\lambda_{app} = V_{app} / f_{input}$, and $\lambda_{soil} = V_s / f_{input}$. V_{app} is a parameter often used to control the wave passage effect. It is obtained combining the shear wave velocity of the soil deposit (V_s) with the angle of inclination of the incoming waves with the following relationship:

$$V_{app} = \frac{V_s}{\sin \vartheta} \quad (2)$$

where ϑ is the inclination of the incoming waves from the vertical direction. Small values of $\lambda_{app} / \lambda_{soil}$ correspond to severe SVGM, while when $\lambda_{app} / \lambda_{soil}$ tends to infinity, the response tends to the synchronous motion (i.e., no wave passage effects).

In order to ensure the numerical accuracy of the wave transmission processes (Kuhlemeyer and Lysmer 1973), the mesh always comprises elements smaller than one-tenth of the wavelength of the highest frequency component of the input.

4 Model verification

The numerical model presented in the previous section is verified using numerical solutions available in literature for canyons with regular shapes that consider undamped elastic uniform soil and vertically propagating harmonic SV waves. As mentioned

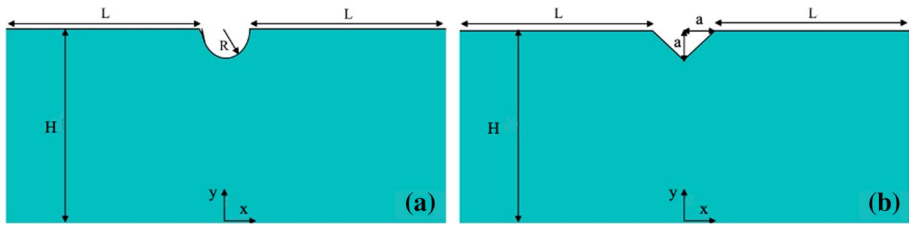


Fig. 3 Definition of the geometric parameter for: **a** semi-circular, and **b** symmetric V-shaped canyons

in the previous section, three canyons are considered in this study: (i) semi-circular canyon shape (Fig. 3a), verified against the solution proposed by Wong (1982), and a Boundary Element Method (BEM) solution (Ausilio et al. 2008; Ausilio and Zimmaro 2012); (ii) symmetric triangular canyon shape (Fig. 3b), verified against BEM (Ausilio et al. 2008) and FEM solutions (Godinho et al. (2009)); (iii) the actual geometry of the Lao River canyon (Fig. 2), verified against a BEM solution specifically implemented for this study. The input is formed by sinusoidal (harmonic) vertically-incident SV waves formed by 5 ramp-up, 30 stationary, and 5 ramp-down cycles. The analyses include a broad range of dimensionless frequencies (η), defined as:

$$\eta = \frac{\omega R_0}{\pi V_s} \quad (3)$$

where ω is the angular frequency of the input, R_0 is the representative geometric parameter of the canyon ($R_0 = R = 25$ m for semi-circular canyon, $R_0 = a = 25$ m for symmetric triangular canyon, and $R_0 = B = 100$ m for the Lao River canyon) and V_s is the shear wave velocity of the soil ($V_s = 500$ m/s in all the analyses). No material damping was used, whereas numerical damping is included in the analyses to ensure numerical stability.

Results of the verification process are presented in terms of horizontal (U_h) and vertical (U_v) components of the peak ground surface displacement. All quantities are normalized by the input amplitude for three values of the dimensionless frequency η (0.5, 1.0, and 1.5). The verification also includes the extension of the model, parametrized using the ratio of the lateral extension of the model (L) and its height (H), to verify the performance of the boundary conditions adopted herein.

Figures 4 and 5 show the comparison of the results obtained from the FEM OpenSees model with the solutions available in the literature for semi-circular and V-shaped canyons, respectively. Results are plotted using a normalized distance from the center of the canyon, computed as X/R_0 . Figures 4 and 5 show that the agreement between the FEM model and the literature solutions is satisfactory. The extension of the model influences the vertical amplification more than that in the horizontal direction. Increasing L/H leads to more accurate results only for the semi-circular canyon (Fig. 4 with $\eta = 1$), while the difference between $L/H = 5$ and $L/H = 6$ is not significant for the V-shaped canyon (Fig. 5). For this reason, the models with $L/H = 6$ is used for the parametric analysis for both semi-circular and V-shaped canyons.

Figure 6 shows the comparison between the FEM model presented in this study and the BEM solution implemented in this paper for the Lao River canyon overcrossed by the Viadotto Italia. The agreement between the two models is always satisfactory, and

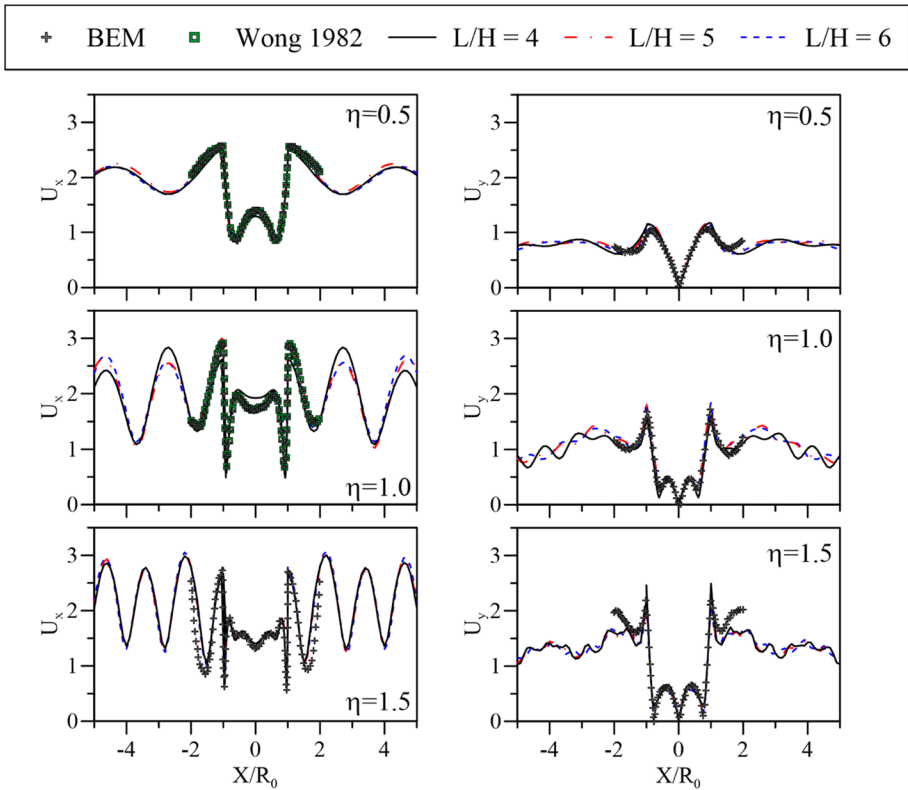


Fig. 4 Semi-circular shaped canyon: comparison of the proposed FEM model with the available solutions for horizontal (U_x) and vertical (U_y) components at surface versus the normalized distance from the center of the model (X/R_0)

the lateral extent of the model is not influencing the accuracy of the response. For this reason, to minimize the computation effort, the smaller Lao River canyon model with $L/H=4$ is used in all the analyses presented in the following section.

5 Parametric analysis

A parametric analysis is performed to analyze the effect of the combination of the topographic irregularities with wave passage effects. For each canyon, V_{app} is used to compute the delay (Δt) induced by the inclination of the upcoming waves associated with the SVGM. The range of variability of $\lambda_{app}/\lambda_{soil}$ considered in this study is from 1 to 10, corresponding to an inclination of the upcoming waves from 90° to 5.7° , respectively (Fig. 7). All the analyses are performed using three different values of the dimensionless frequency: 0.5, 1.0, and 1.5. The influence of the direction of the upcoming waves is also included in this study, considering the cases of waves coming from left to right and from right to left. The input considered in all the analyses is formed by a sinusoidal vertically-incident SV waves.

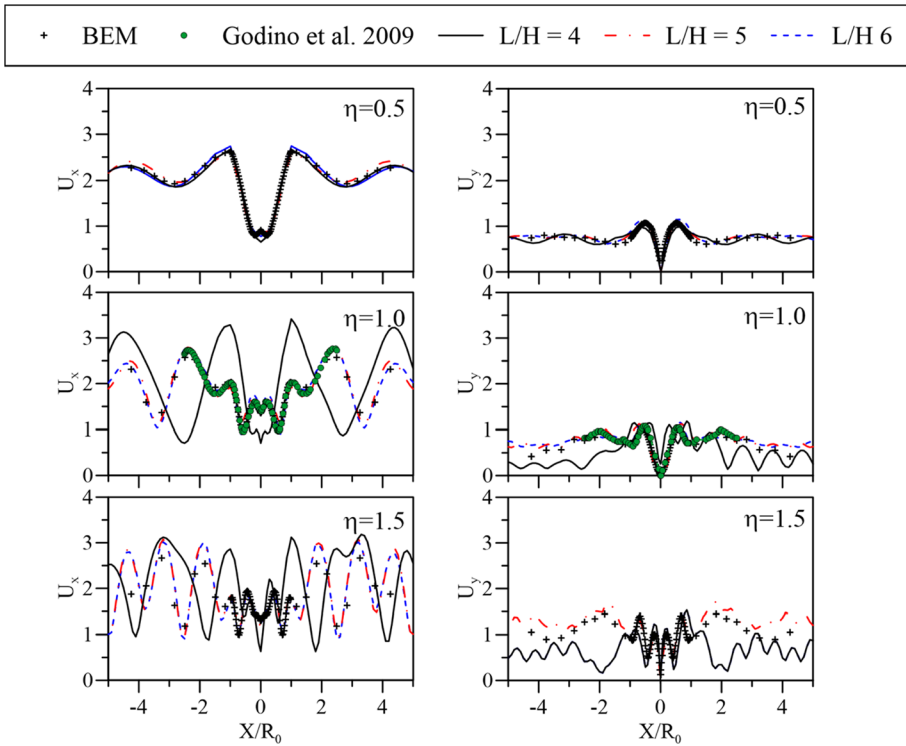


Fig. 5 Symmetric V-shaped canyon: comparison of the proposed FEM model with the available solutions for horizontal (U_x) and vertical (U_y) components at surface versus the normalized distance from the center of the model (X/R_0)

Results along the surface of the canyon are presented in terms of horizontal (A_h) and vertical (A_v) aggravation factors (Assimaki et al. 2005). They are defined as the ratio between the peak ground acceleration at the top of the topographic irregularity (horizontal and vertical component, respectively) and the horizontal peak ground acceleration in free-field conditions.

5.1 Semi-circular canyon

Figure 8 shows the results for the semi-circular shaped canyon for $\eta = 1.0$ considering waves coming in the soil deposit from left to right. The comparison between the synchronous motion (black) and the asynchronous motion (colored lines) shows how different the response of the model is when considering the wave passage effect of the upcoming waves. The variation of A_h along the surface of the canyon shows how different in amplitude and shape the response is compared against the synchronous motion. With reference to the synchronous motion (NO WPE), all the models with $\lambda_{app}/\lambda_{soil} > 2$ tend to amplify the horizontal component and to de-amplify the vertical component on the side from which waves are coming (i.e., the left side if waves are traveling left to right), and vice-versa on the second half of the soil deposit. This behavior is more evident in Fig. 9, where A_h and A_v at three control points (at the beginning, center, and

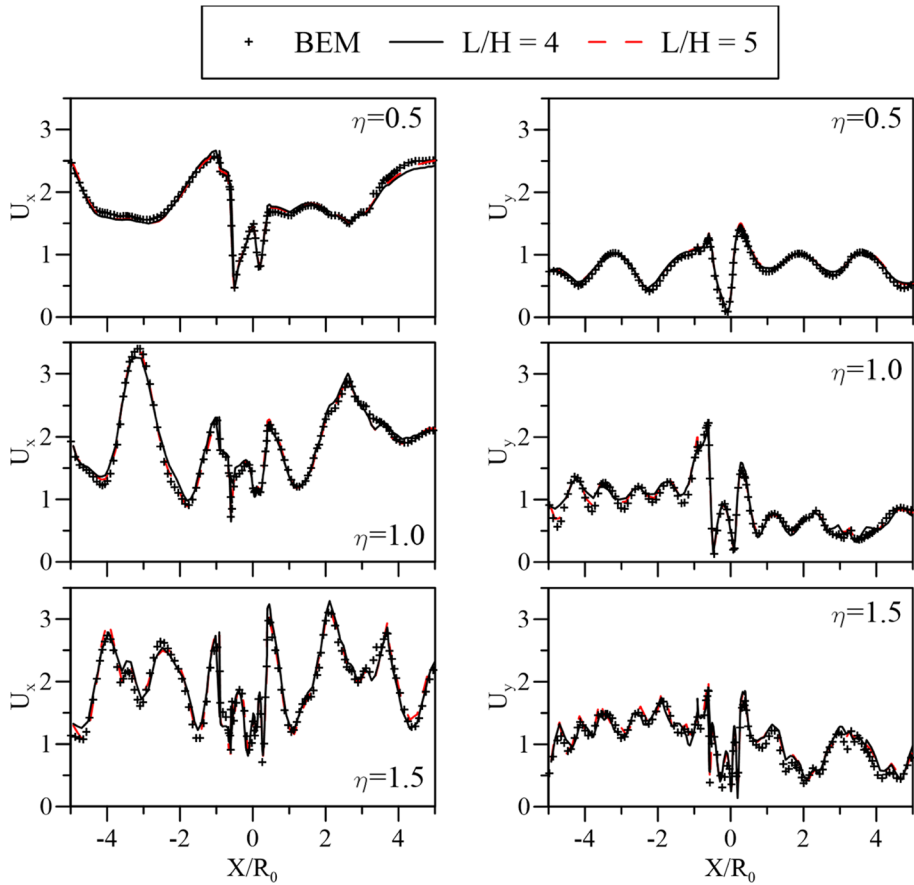


Fig. 6 Lao River canyon: comparison of the proposed FEM model with an *ad-hoc* BEM solution for horizontal (U_x) and vertical (U_y) components at surface versus the normalized distance from the center of the model (X/R_0)

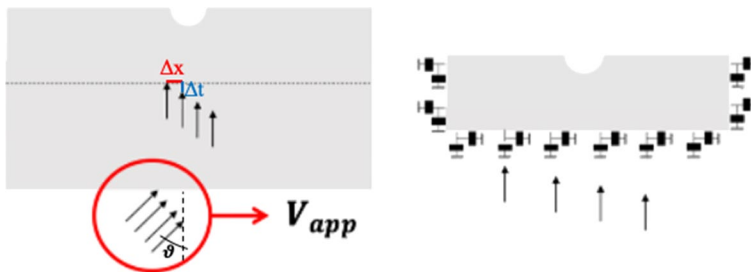


Fig. 7 Schematic of the wave passage effect

end of the topographic feature) are reported for each value of $\lambda_{app}/\lambda_{soil}$ for values of the dimensionless frequency equal to 0.5, 1.0, and 1.5. All the dimensionless frequencies considered show how the directionality of the waves tends to generate an amplification

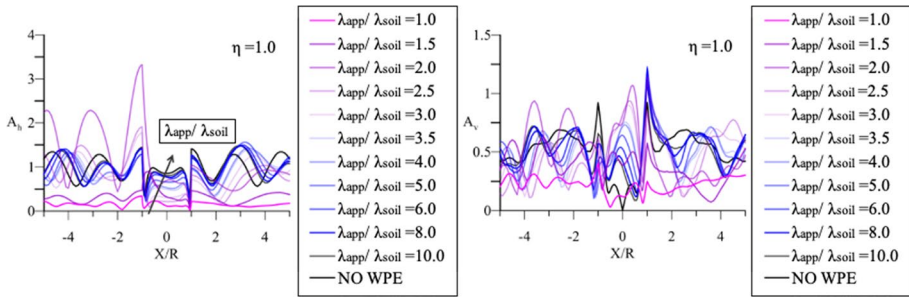


Fig. 8 Horizontal (A_h) and vertical (A_v) aggravation factors along the surface of the canyon for the semi-circular shaped canyon for different values of $\lambda_{app}/\lambda_{soil}$ ($\eta=1.0$, waves travelling from left to right) versus the normalized distance from the center of the model (X/R)

around $\lambda_{app}/\lambda_{soil} = 2$, that corresponds to an inclination of 30° . This inclination was already been recognized as a critical inclination for canyons by previous studies (e.g., Ashford and Sitar 1997). As expected, both the horizontal and vertical aggravation factors tend to the value obtained for the synchronous motion for high values of $\lambda_{app}/\lambda_{soil}$ (a theoretical infinite ratio corresponds to the synchronous motion).

Figure 10 shows A_h and A_v along the surface of the canyon considering the two opposite directions for the incoming waves (from left to right, solid red line, and from right to left, dashed red line) for the most severe condition ($\lambda_{app}/\lambda_{soil} = 2$ and $\eta = 1$). The wave passage effect eliminates the symmetry in the response observed for the synchronous motion (solid black line), generating a concentration of the horizontal waves (and increasing amplitude) and a de-amplification of the vertical waves on the side of the canyon where the waves arrive first, and vice-versa. Furthermore, the wave passage effect generates a non-zero vertical amplification in correspondence to the center of the canyon. Similar effects related to the direction of the motion were observed for V-shaped canyons and are reported in the following section.

5.2 V-shaped canyon

Figure 11 shows the results for the V-shaped canyon for $\eta = 1.0$ considering waves travelling from left to right. The comparison between the synchronous motion (in black) and the complete SVGM (colored lines) shows the same trend observed for the semi-circular shaped canyon. The highest horizontal and vertical amplifications happen for $\lambda_{app}/\lambda_{soil} = 2$, at the first (beginning of the canyon) and last (end of the canyon) reference points, respectively.

Figure 12 shows the variation of A_h and A_v for each dimensionless frequency considered at the three reference points. Differently to what observed for the semi-circular shaped canyon, the peak in the aggravation factors is more evident in the vertical component. Again, as expected, all the plots in Fig. 12 tend to the values obtained for the synchronous motion for high $\lambda_{app}/\lambda_{soil}$ ratios.

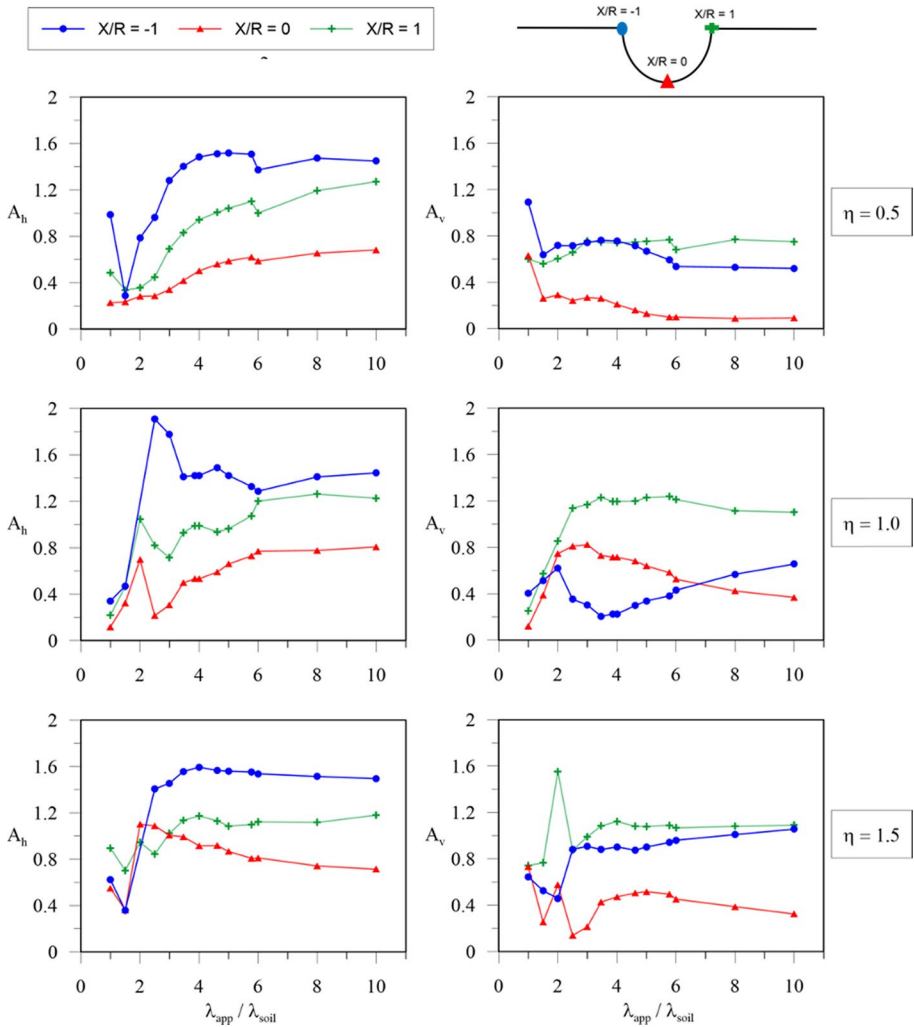


Fig. 9 Variation of horizontal and vertical aggravation factors at three control points with $\lambda_{app}/\lambda_{soil}$ for dimensionless frequency values equal to 0.5, 1.0, and 1.5 for the semi-circular shaped canyon

5.3 Lao River (Viadotto Italia) canyon

Figure 13 shows the variation of the horizontal and vertical aggravation factors along the surface for the Lao River canyon, for synchronous and asynchronous input motions excited with a dimensionless frequency equal to one with waves from left to right. A_h and A_v present variation in amplitude that is always less than 2, and the trend observed for regularly-shaped canyons with $\lambda_{app}/\lambda_{soil}$ is not as clear. Nevertheless, the alternance of amplification and de-amplification of the motion for points nearby (i.e., successive bridge pier locations), generates strong stresses onto the superstructure. Such effect should be considered in future simplified and/or advanced soil-structure interaction models for long multi-span bridges.

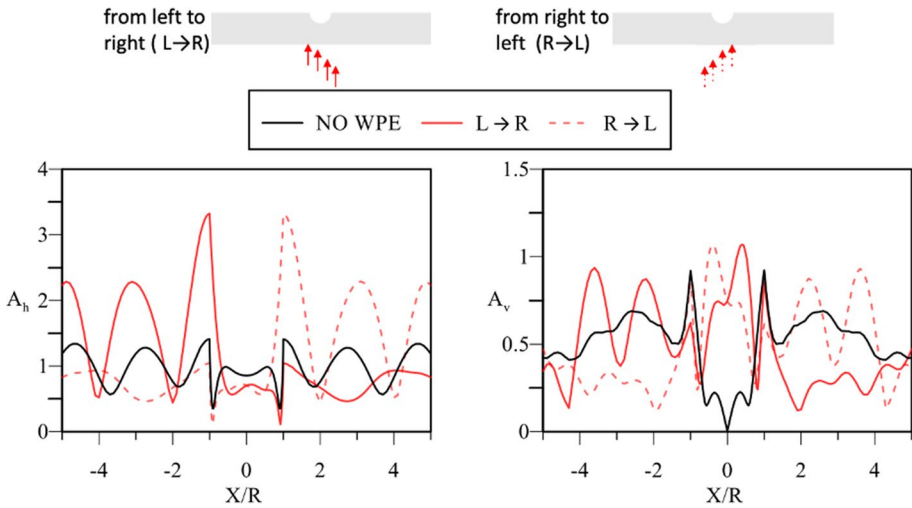


Fig. 10 Horizontal (A_h) and vertical (A_v) aggravation factors variation along the surface of the canyon considering waves travelling from left to right (solid red line) and from right to left (dashed red line) for $\lambda_{app}/\lambda_{soil} = 2$ and $\eta = 1$ versus the normalized distance from the center of the model (X/R)

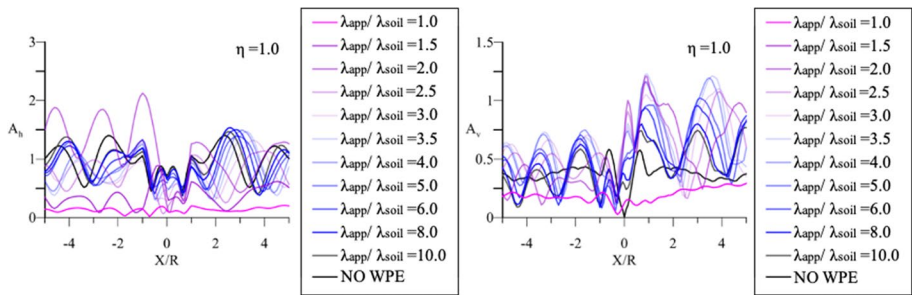


Fig. 11 Horizontal (A_h) and vertical (A_v) aggravation factors along the surface of the canyon for the V-shaped canyon for different values of $\lambda_{app}/\lambda_{soil}$ ($\eta = 1.0$, waves travelling from left to right) versus the normalized distance from the center of the model (X/R)

Figure 14 shows the variation of A_h and A_v for the three dimensionless frequencies considered (0.5, 1.0, and 1.5) in correspondence of four control points (P4, P5, P6, and P7). The control points selected are the locations of the four center piers, that represent the most vulnerable elements of the bridge. With reference to A_h , P4 and P5 show a synchronous response for $\lambda_{app}/\lambda_{soil}$ less than three, while they have an opposite behavior for higher values of $\lambda_{app}/\lambda_{soil}$. P7 shows de-amplification effects for all asynchronous cases. Comparing the response in correspondence of all control points, it is possible to notice how at all locations, the trend observed for $\eta = 0.5$ is kept for $\eta = 1.0$. Such trend is inverted (becoming the opposite) once the resonant condition is passed ($\eta = 1.5$).

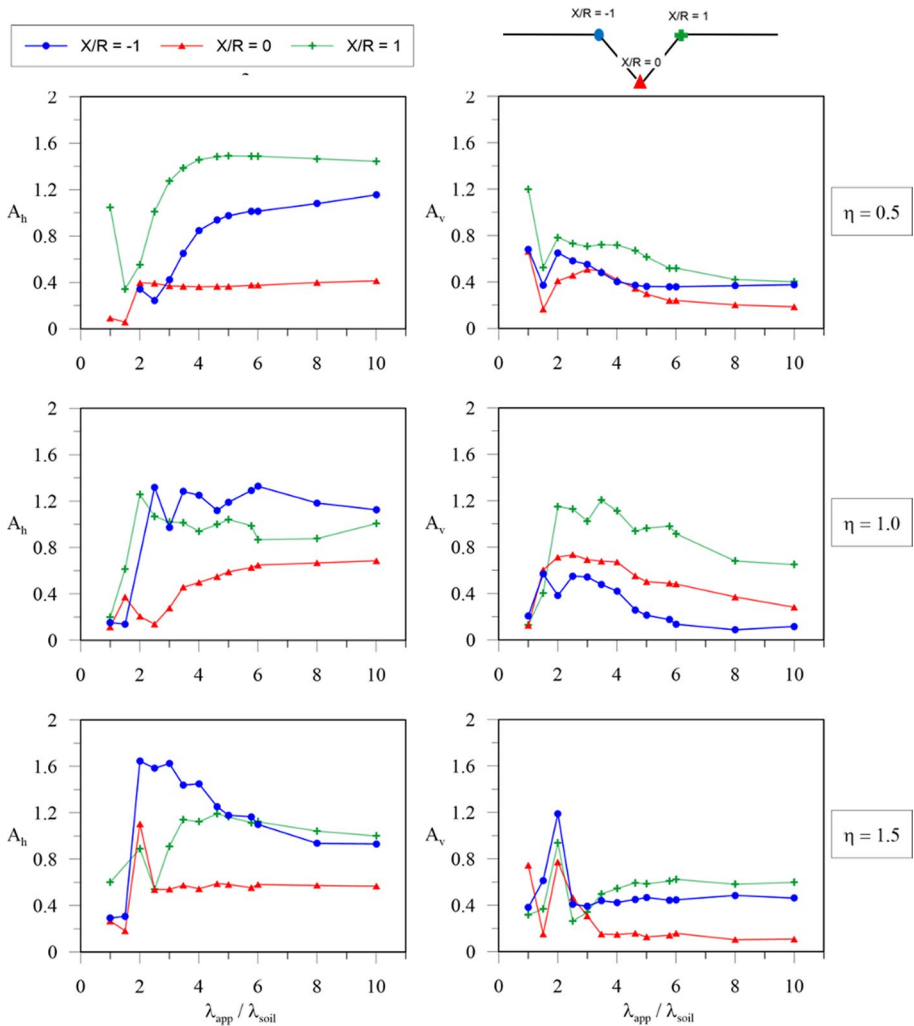


Fig. 12 Variation of horizontal and vertical aggravation factors at three control points with $\lambda_{app}/\lambda_{soil}$ for dimensionless frequency values equal to 0.5, 1.0, and 1.5 for the V-shaped canyon

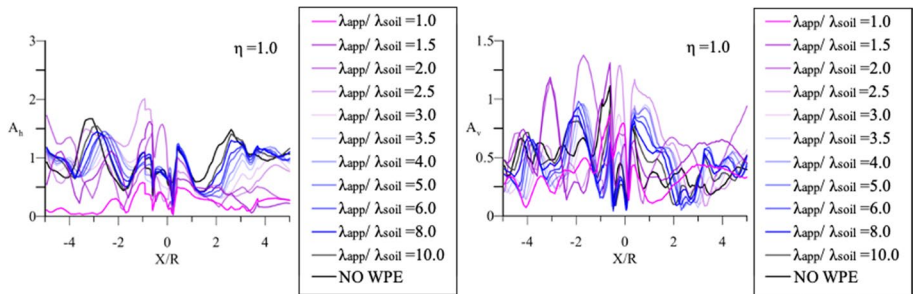


Fig. 13 Horizontal (A_h) and vertical (A_v) aggravation factors along the surface of the canyon for the Lao River canyon for different values of $\lambda_{app}/\lambda_{soil}$ ($\eta = 1.0$, waves travelling from left to right) versus the normalized distance from the center of the model (X/R)

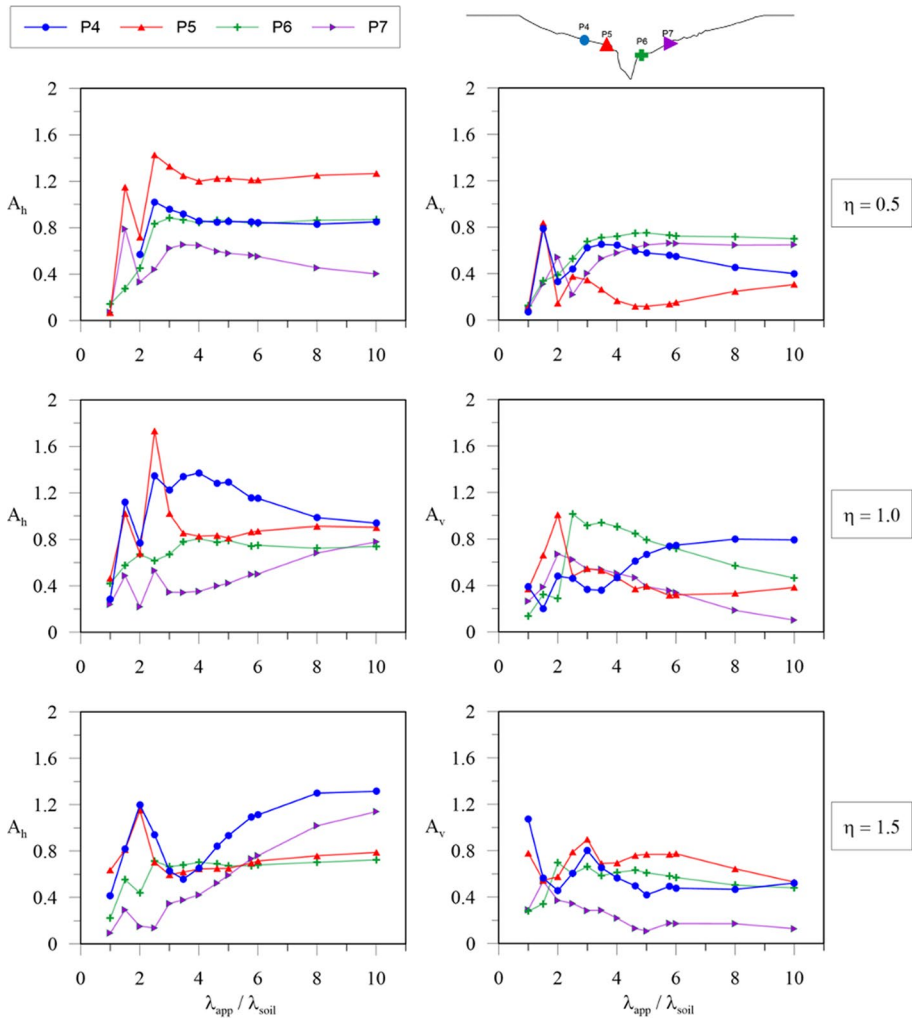


Fig. 14 Variation of horizontal and vertical aggravation factors at the principal reference points with $\lambda_{app}/\lambda_{soil}$ for dimensionless frequency equal to 0.5, 1.0, and 1.5 for the Lao river canyon

6 Conclusions

This paper presented an exploration of the combined effect of wave passage and differently-shaped 2D topographic features on the spatial variation of the ground motion. The analysis was conducted using a large number of FEM numerical simulations. The FEM model used in this study was verified against known analytical and numerical solutions and ad-hoc numerical models. We analyzed two regularly-shaped canyons (semi-circular and V-shaped), and a real canyon (the Lao River canyon crossed by the Viadotto Italia—a long multi-span bridge) located along the A2 highway in Southern Italy. The effect of the spatial variation of the ground motion has been analyzed including both topographic irregularities and the wave passage effect into the numerical model. Such combined effect was

obtained by directly modeling topographic features and adding a delay to the input motion to account for wave passage. Geometric incoherence and 1D ground response effects (due to the presence of different soil layers) of the input are neglected in this study to focus on how the combination of wave passage and topographic effects modify the input motion. Such choice is justified by the need of explicitly accounting for site effects, often neglected or treated with simplified approaches in existing engineering models.

The analyses shown in this paper mainly focus on amplification/deamplification phenomena caused by the combined effect of topographic irregularities and the wave passage effect. However, we recognize that phase lag is also an important aspect of this problem. Insights into this issue are addressed by Durante et al. (2018) for some of the geometries analyzed in this study. The parametric analysis we performed showed that when topographic irregularities are present, the wave passage effect can significantly modify the soil response of both the horizontal and vertical components of the surface motion. Furthermore, the vertical component of the surface acceleration can become comparable, or even larger than the horizontal components. The surface acceleration turns out to be strongly affected by the shape of the canyon, and it is not possible to define a-priori the severity of the combined effect of topographic irregularities and wave passage. This suggests, that both effects should be analyzed together as they cannot be simply uncoupled (or neglected). The analysis of the effect of the travelling direction of the incoming waves showed that the response is specular for symmetric canyons. This path effect has different trends for non-symmetric canyons and should be always considered taking into account the direction of incoming waves. Such information can be supplemented by seismological studies and/or the definition of scenario events.

References

- Abrahamson NA, Schneider JF, Stepp JC (1991) Empirical spatial coherency functions for applications to soil structure interaction analyses. *Earthq Spectra* 7:1–27
- Ashford AS, Sitar N (1997) Analysis of topographic amplification of inclined shear waves in a steep coastal bluff. *Bull Seismol Soc Am* 87(3):692–700
- Assimaki D, Gazetas G, Kausel E (2005) Effects of local soil conditions on the topographic aggravation of seismic motion: parametric investigation and recorded field evidence from the 1999 Athens earthquake. *Bull Seismol Soc Am* 95:1059–1089
- Assimaki D, Gazetas G (2004) Soil and topography amplification on canyon banks and the 1999 Athens earthquake. *J Earthq Eng* 8(1):1–43
- Assimaki D, Jeong S (2013) Ground-motion observations at Hotel Montana during the M 7.0 2010 Haiti earthquake: topography or soil amplification? *Bull Seismol Soc Am* 103:2577–2590
- Ausilio E, Conte E, Dente G (2008) Seismic response of alluvial valleys to SH waves. In: *Seismic engineering conference, AIP conference proceedings*, vol 1020, pp 199–206. <https://doi.org/10.1063/1.2963835>
- Ausilio E, Zimmaro P (2012) Topographic effects evaluation for performance-based design. In: *Proceedings of 2nd international conference on performance-based design in earthquake geotechnical engineering*, Taormina, Italy
- Capatti MC, Tropeano G, Morici M, Carbonari S, Dezi F, Leoni G, Silvestri F (2016) Implications of multi-support excitation induced by site conditions, non-linear soil behaviour and SSI on the seismic response of long bridges. *Bull Earthq Eng* 15(11):4963–4995. <https://doi.org/10.1007/s10518-017-0165-z>
- Celebi, M, Hanks T (1986) Unique site response conditions of two major earthquakes of 1985: Chile and Mexico. In: *Proceedings of the international symposium of engineering geology problems in seismic areas*, Bari, Italy, vol IV
- Cestelli GC, De Miranda F, Pellegrino GC (1965) Il progetto del viadotto sul fiume Lao dell'Autostrada Salerno-Reggio Calabria. *Acciaio Costr Metall* 6:454–458 ((in italian))
- Davis LL, West LR (1973) Observed effects of topography on ground motion. *Bull Seismol Soc Am* 63:283–298

- Durante MG, Brandenberg SJ, Ausilio E, Zimmaro P (2018) Influence of topographic irregularities on the asynchronism of strong ground motions. In: 11th national conference on earthquake engineering, Los Angeles, CA, USA
- Elanashai AS, Borzi B, Vlachos S (1999) Deformation-based vulnerability functions for RC bridges. *Struct Eng Mech* 17(2):215–244
- Godinho L, Amado MP, Tadeu A, Cadena-Isaza A, Smerzini C, Sánchez-Sesma FJ, Madec R, Komatitsch D (2009) Numerical simulation of ground rotations along 2D topographical profiles under the incidence of elastic plane waves. *Bull Seismol Soc Am* 99(2B):1147–1161
- Harichandran RS, Vanmarcke EH (1986) Stochastic variation of earthquake ground motion in space and time. *J Eng Mech ASCE* 112(2):154–174
- Kuhlemeyer RL, Lysmer J (1973) Finite element method accuracy for wave propagation problems. *J Soil Dyn Div ASCE* 99:421–427
- Luco JE, Wong HL (1986) Response of a rigid foundation to a spatially random ground motion. *Earthq Eng Struct Dyn* 14:891–908
- Lupoi A, Franchin P, Pinto PE, Monti G (2005) Seismic design of bridges accounting for spatial variability of ground motion. *Earthq Eng Struct Dyn* 34:327–348
- Lysmer J, Kuhlemeyer RL (1969) Finite dynamic model for infinite media. *J Eng Mech Div, ASCE*, 95(EM4):859–877
- McKenna F, Fenves GL (2005) The OpenSees command language manual, version 2.5. Pacific Earthquake Engineering Research Center, University of California, Berkeley. <http://opensees.berkeley.edu>
- Nuti C, Vanzi I (2005) Influence of earthquake spatial variability on differential soil displacements and SDF system response. *Earthq Eng Struct Dynam* 34:133–1374
- Park D, Sagong M, Kwak DY, Jeong CG (2009) Simulation of tunnel response under spatially varying ground motion. *Soil Dyn Earthq Eng* 29:1417–1424
- Sextos AG, Ptilakis D, Kappos AJ (2003) Inelastic dynamic analysis of RC bridges accounting for spatial variability of ground motion, site effects and soil structure interaction phenomena. Part 1: methodology and analytical tools. Part 2: parametric study. *Earthq Eng Struct Dyn* 32(4):607–652
- Sextos AG, Ptilakis D, Kappos A (2005) Evaluation of the new Eurocode 8-part 2 provisions regarding asynchronous excitation of irregular bridges. In: 4th European workshop on the seismic behaviour of irregular and complex structures, Thessaloniki, Paper no. 04
- Siro L (1982) Southern Italy November 23 1980 earthquake. In: Proceedings of the 7th European conference on earthquake engineering, Athens, Greece
- Trifunac MD (1973) Scattering of plane SH waves by a semi-cylindrical canyon. *Earthq Eng Struct Dynam* 1:267–281
- Vanmarcke EH (1983) Random fields: analysis and synthesis. MIT press, Cambridge, pp 247–264
- Wong HL (1982) Effect of surface topography on the diffraction of P, SV and Rayleigh waves. *Bull Seismol Soc Am* 72:1167–1183
- Wu Y, Gao Y, Zhang N, Li D (2016) Simulation of spatially varying ground motions in V-shaped symmetric canyons. *J Earthq Eng* 20(6):992–1010
- Zerva A (1990) Response of multispan beams to spatially incoherent seismic ground motions. *Earthq Eng Struct Dyn* 19:819–832
- Zhang Y, Yang Z, Bielak J, Conte EJP, Elgamal A (2003) Treatment of seismic input and boundary conditions in nonlinear seismic analysis of a bridge ground system. In: 16th ASCE engineering mechanics conference, July 16–18, 2003. University of Washington, Seattle

Publisher's Note Springer Nature remains neutral with regard to jurisdictional claims in published maps and institutional affiliations.